RSC Advances

ROYAL SOCIETY OF CHEMISTRY

www.rsc.org/advances

Sensitive sandwich electrochemical immunosensor for human chorionic gonadotropin using nanoporous Pd as label

Yiming Liu, Wenjuan Guo*, Xiaoli Qin, Xue Meng, Xiangwei Zhu, Jinping Wang, Meishan Pei, Luyan Wang

Shandong Provincial Key Laboratory of Chemical Sensing & Analysis, School of Chemistry and Chemical Engineering, University of Jinan, Jinan 250022, China

*Corresponding author. Tel: +86-15689733522

E-mail address: chm_guowj@163.com

Abstract

A novel sandwich-type electrochemical immunosensor for sensitive detection of human chorionic gonadotropin (hCG) was designed. The nanoporous Pd (NP-Pd) was prepared by dealloying method and used as electrochemical label due to its wonderful conductivity, good biocompatibility and strong electrocatalytic activity toward antigen-antibody reaction. Results proved that the immunosensor fabricated using the label based on NP-Pd loaded with horseradish peroxidase (HRP) and secondary anti-hCG antibody (Ab_2) (NP-Pd-HRP-Ab_2) had high sensitivity, and the sensitivity of the label NP-Pd-HRP-Ab_2 was much higher than that of HRP-Ab_2. Gold nanoparticles (GNPs), Prussian blue (PB) and GNPs as immobilization matrix were not only used to immobilize anti-hCG (Ab_1) but also took part in the signal amplification. Under optimized condition, the amperometric signal increased linearly with hCG concentration in the range of 0.5 ng/mL to 200 ng/mL (γ =0.9986) with a low detection limit (3σ) of 9.2 pg/mL (0.093 mIU/mL). The immunosensor displayed good sensitivity and selectivity. In addition, the immunosensor was successfully used for the determination of hCG in human serum.

Introduction

Human chorionic gonadotropin (hCG), a highly glycosylated protein (37.5 kDa), is produced in pregnancy[1]. During pregnancy, the variation of hCG in the urine or serum of human can cause some diseases, such as ovarian cancer, chorioepithelioma and male sterility. Therefore, there is a pressing need to develop a device that can rapidly measure the hCG concentration.

Currently, many analytical techniques were described in the literature, such as radioimmunoassay[2-4], luminescence immunoassay[5-7], fluoroimmunoassay[8-12] spectrometry[13], resonance scattering spectral assay[14] and electrochemical immunosensors[15-17]. Among these techniques, electrochemical immunosensors[18-21] have been proved to be ideal methods due to their inherent advantages, such as the high sensitivity, low cost, easy of miniaturization, simple pretreatment procedures, fast analytical time, precise measurement, and small-sized instruments. Moreover, sandwich-type electrochemical immunosensors[22-24] have gained much attention because of their high specificity and sensitivity. In the process of the design and fabrication of highly sensitive electrochemical immunosensors, signal amplification, antibody (Ab)/antigen (Ag) immobilization and noise reduction are the crucial steps. In general, noise can be reduced by reducing the background current of the as-prepared immunosensor. Signal amplification and Ag immobilization can be improved by using nanoparticles.

Nowadays, particular attention has been paid to nanoparticles[25] with the rapid development of nanotechnology. Nanoparticles are used as labels or to modify

electrode to amplify signal. Various nanomaterials including gold nanoparticles (GNPs)[26-28], graphite[29], carbon nanotube[30-34] have been reported in immunosensors. Meanwhile, it has been demonstrated that nanoporous metals with three-dimensional pore-ligament structure obtained by simple dealloying have special physicochemical properties[35, 36] and Pt (Pd)-based catalysts are very important in green-energy technologies and industrial catalysis. The catalytic activity of Pd nanomaterials has been extensively investigated[37-39]. In addition, Pd is cheaper compared with other materials, such as Au and Pt. Nanoporous Pd (NP-Pd), prepared using dealloying method, not only provides the higher surface area for the conjugation of antibody but also facilitates the electron transfer. The surface of NP-Pd prepared in alkaline solution (without any surfactants) is extremely clean, and NP-Pd can be easily employed. Therefore, NP-Pd is believed to offer unprecedented benefits in catalysis design.

In this study, a novel sandwich-type immunosensor was successfully prepared to detect hCG. Firstly, GNPs/Prussian blue (PB)/GNPs nanocomposites were modified onto the electrode surface in order to immobilize hCG Ab_1 then capture Ag, based on which the amount of the immobilized Ab_1 was enlarged and the current response of the electrode enhanced. Secondly, the synthesized NP-Pd was employed as the carrier for HRP-Ab_2. HRP-Ab_2-NP-Pd bioconjugates were used as a second signal amplification strategy. The aim of this work is to employ advanced nanoporous materials (NP-Pd) as a carrier to fabricate a highly sensitive, selective, and simple sandwich-type immunosensor for detecting hCG. The as-prepared immunosensor may

provide potential applications for the ultrasensitive detection of different biomolecule.

Reagent and materials

Materials and methods

Reagents

Ag, hCG antibody (Ab_1, HRP-Ab_2), carcinoembryonic antigen (CEA) and alfa fetoprotein (AFP) were purchased from Shanghai Lingcao Biotechnology Co., Ltd. (China). Gold chloride ($HAuCl_4 \cdot 4H_2O$), bovine serum albumin (BSA), folic acid, ascorbic acid (Vc) and L-glutamic acid were purchased from Sinopharm Chemical Reagent Co., Ltd. (China). Other chemicals and solvents were of guaranteed analytical grade. Ultrapure water was used throughout this study.

Apparatus

All electrochemical measurements were performed on Zennium electrochemical workstation (Zahner, Germany). The micro-structures of NP-Pd were characterized on a QUANTA PEG 250 scanning electron microscope (SEM) and a JEM-2100 high resolution transmission electron microscopy (HRTEM). The Barunauer-Emmett-Teller (BET) analyses were using nitrogen adsorption instrument (America, Quantachrome). Grain size distribution of NP-Pd were tested by using laser partical size analyzer (Britain, Malvern).

Electrochemical measurements were performed using a three-electrode system composed of a modified glassy carbon electrode (GCE) as working electrode, a platinum wire as counter electrode, and Ag/AgCl as reference electrode. All electrochemical measurements were done in an unstirred electrochemical cell at room

temperature.

Synthesis of NP-Pd

The NP-Pd was prepared according to literature[40]. PdAl alloy foils were made by refining pure (>99.9%) Pd and Al under the protection of argon atmosphere in a furnace, followed by melt-spinning. Then the NP-Pd was gained by dipping PdAl alloy foils in NaOH solutions at room temperature for 24 h. During the dealloying process, Pd atoms left behind would self-organize into an interconnected network of pores and ligaments. After dealloying, the foils were crushed to uniformed grain.

Bioconjugation of nanoporous Pd with HRP-Ab_2

5 mg NP-Pd was initially added into 1 mL PBS (0.1M, pH 7.2) and sonicated 5 min to obtain a homogeneous dispersion. 100 μL HRP-Ab_2 (1 mg mL^{-1}) was injected into the mixture and incubated for 12 h at 4 □. The residual antibody was removed by centrifugation. Then the precipitate was washed with 0.1 M PBS for three times and immersed in 1% BSA solution for 1h at 4 □ to block the remaining active groups and eliminate nonspecific binding effect. The resulting mixture was centrifuged and washed with PBS for several times. The prepared HRP-Ab_2-NP-Pd was then stored in PBS (0.1 M, pH 7.2) at 4 □ until use.

Preparation of the modified electrode

The GCE was polished to a mirror finish with 0.3 and 0.05 μm alumina slurry, and then thoroughly washed ultrasonically in ethanol and ultrapure water in turn. The cleaned electrode was soaked in $HAuCl_4$ aqueous solution (1%, w/w) and electrodeposited at -0.2 V for 300 s to get a GNPs layer. The preparation of PB/ GNPs

/GCE was accomplished in aqueous solution containing 2.5 mM $FeCl_3$, 2.5 mM $K_3[Fe(CN)_6]$, 0.1 M HCl and 0.1 M KCl by applying a constant potential of 0.4 V for 400 s. Following that, electrodeposition was performed in $HAuCl_4$ solution (1%, w/w) at potential of -0.2 V for 5 min again. After that, the GNPs/PB/GNPs/GCE was obtained.

Preparation of electrochemical immunosensor

The modified working electrode was incubated with Ab_1 for 12h, followed by washing with PBS to remove nonspecific physically adsorption. Then the modified electrode was immersed in 1% BSA solution for 1h at 4 □ to block nonspecific binding sites between the Ab_1 and the electrode surface. Subsequently, the electrode was incubated in a varying concentration of hCG solution for 2 h. Finally, 10μL of the prepared HRP-Ab_2-NP-Pd solution was dropped onto the electrode surface and incubated for an additional 1 h. Each step was washed by PBS thoroughly for several times. The schematic diagram of the stepwise procedure of the immunosensor was shown in Scheme 1.

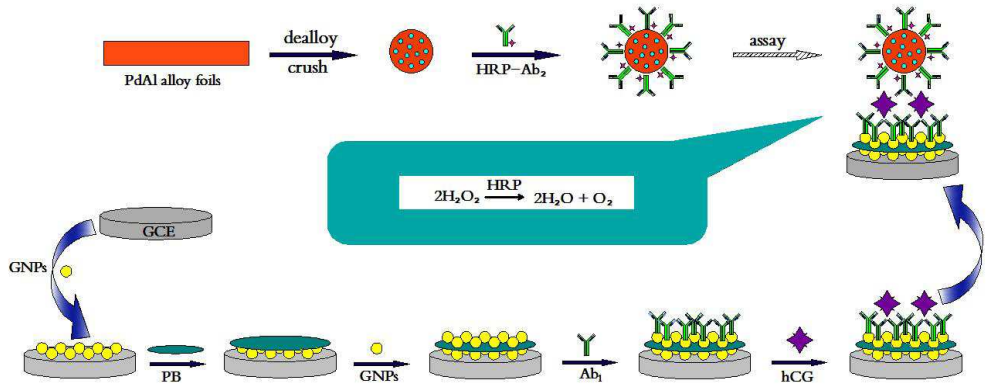

Scheme. 1. Illustration of the stepwise immunosensor fabrication process.

Results and discussion

Characterization of NP-Pd

NP-Pd sample was tablet for SEM (Fig. 1(A)). It is clear that the dealloyed sample consists of a number of uitrafine nanoporous. Meanwhile, NP-Pd sample was dispersed in solvent, and then it was further confirmed by HRTEM. Fig. 1(B) showed HRTEM image of NP-Pd sample. The clear contrast between the bright regions and the dark skeletons further confirms the formation of a three-dimensional (3D) interconnected network structure on the nanoscale, which is beneficial for the mass and electron transport during electrochemical sensing. It is consistent with the SEM observation. The energy dispersive X-ray spectrum (EDS) (Fig. 1(C)) proved that the nanoporous material is composed of Pd with a small amount of residual Al. Pore size ditributions were determined by BET analyses for NP-Pd. The pore diameter of NP-Pd was 5.1 nm as shown in Fig. 1(D). Meanwhile, the grain size distribution were tested (Fig. 1(E)). The average size of grain was 88.6 nm. These results indicate that NP-Pd was fabricated by means of a simple dealloying procedure. This method is in sharp contrast to the traditional approach, and this method can achieve a nearly 100% yield.

Characterization of immunosensor

The characteristics of the differently modified electrodes were measured by CVs after each assembly step. In Fig. 2, after coated with the mixture of GNPs and PB, the current response of the electrode in PBS containing $K_3[Fe(CN)_6]$ was apparently larger than that of the bare electrode. The higher current response might be attributed to dual-amplification effects of the GNPs and PB. GNPs with good conductivity

increased the effective surface area of the electrode. PB, which has the formula $Fe^{3+}[Fe^{2+}(CN)_6]_3$, is a prototype of metal hexacyanoferrates and could be used as the electron transfer mediator due to electrochemical activity, fine redox reversibility and stability. Moreover, the addition of PB could prevent the leakage of GNPs. On the contrary, when Ab_1 was immobilized on the GNPs/PB/GNPs modified electrode surface, the peak currents decreased. Subsequently, the peak currents decreased after the Ab_1/GNPs/PB/GNPs/GCE reacted with hCG. When Ag/Ab_1/GNPs/PB/GNPs/GCE reacted with HRP-Ab_2-NP-Pd, the peak current further decreased, which demonstrated that hCG and antibody were successfully immobilized on the electrode surface. The reason might be the fact that the fact that hCG antigen and anti-hCG, as biomacromolecules, have weak conductivity, so as to hinder the diffusion of the redox marker toward the electrode surface, hinder electron transfer and insulate the electrode. It could be deduced that the proposed sandwich-type immunosnesor was successfully fabricated from the above results.

Signal amplification via catalytic reduction of H_2O_2 by NP-Pd

To further investigate whether the as-prepared NP-Pd could improve the analytical property of the electrochemical immunoassay, 100 ng mL^{-1} and 150 ng mL^{-1} of hCG antigen were analyzed using the GNPs/PB/GNPs modified electrodes by immunoreacting with either HRP-Ab_2 or HRP-Ab_2-NP-Pd. Fig. 3 displayed the obvious redox peaks of the modified electrodes in PBS (pH 7.2) containing 0.8 mM H_2O_2. The redox peaks might be attributed to the labeled HRP toward the reduction of H_2O_2 and catalytic activity of NP-Pd because of the non-electrochemical activity of

the supporting electrode (PBS). The peak current of HRP-Ab_2-NP-Pd/Ag/Ab_1/GNPs/PB/GNPs modified electrode was increased compared with that of HRP-Ab_2/Ag/Ab_1/GNPs/PB/GNPs modified electrode. The changes of current were 21.67 and 27.3μA at 100 ng mL^{-1} and 150 ng mL^{-1} hCG. The increase was ascribed to the synergistic action between HRP-Ab_2 and NP-Pd. Firstly, NP-Pd with lots of porous could display a high surface-to-volume ratio, which could enhance the immobilized quantity of HRP-Ab_2. Then it provided more chance of the Ag-Ab interaction in turn. Meanwhile, NP-Pd has higher capability of electron transfer. When numerous HRP-Ab_2 were loaded with NP-Pd, NP-Pd could effectively transfer electrons from the base electrode surface to the redox center of HRP. Secondly, the immunosensor exhibited higher catalytic efficiency to the H_2O_2 due to large amounts of HRP. In addition, NP-Pd could catalyze the reduction of H_2O_2, which further enhanced the current response. The results indicated that NP-Pd nanostructures could improve the sensitivity of the electrochemical immunosensors and could be used as an efficient label for ultra-sensitive electrochemical immunnoassay. In addition, Fig. 3 displayed the catalytic current increased with the increase of hCG concentration. The results provided a convenience for detecting hCG.

HRP-Ab2 adsorbed on NP-Pd was quantified by plotting absorbance (A) against the concentration of HRP-Ab2 by ultraviolet spectrophotometry. The linear regression equation: A=0.02585+0.1617c/(mg/L), r=0.9995. The concentration of HRP-Ab_2 in the supernatant （～1mL) was 10.31 mg/L. The results also demonstrated that \ HRP-Ab_2 was successfully loaded with NP-Pd.

Optimisation of the immunoassay conditions

The goal of this study was to obtain the excellent performance of the proposed immunosensor for hCG detection under optimized condition. The current response of the as-prepared immunosensor was directly affected by the quantity and thickness of GNPs and PB. The quantity and thickness of GNPs and PB were decided by the time of electrochemical reaction. The films could be thick, and then hinder the electronic transmission, when the time of electrochemical reaction exceeded a certain value. The CV measurements were carried out in pH 7.2 PBS solution containing 0.2 M KCl and 5 mM $K_3[Fe(CN)_6]$ at a scan rate of 50 mV s^{-1}. As shown in Fig.4 (A), after achieving the maximum current at 300s, the current response decreased, indicating that the optimal reduction time of $HAuCl_4$ was 300s. The time of forming PB film was also studied and the results were shown in Fig.4 (B). The current response reached a maximum at 400s. Therefore, 400s was selected as an optimal time.

In the sandwich-type immunoassays, the pH of the detection solution, the incubation time for the antigen-antibody interaction and the concentration of H_2O_2 also influenced the sensitivity of the as-synthesized immunosnesor. The influence of pH was investigated and the results were shown in Fig.4 (C). The current response decreased at strong acidic and alkaline solution. The optimal response was obtained at pH 7.2. The reason is that the pH of the detection solution might influence not only the catalytic potential of activity of HRP and the bioactivity of immobilized immunoproteins, but also the electrochemical performance of GCE. Therefore, a pH 7.2 of the working buffer was applied for further experiments.

The incubation time between Ab and Ag was an important parameter for capturing hCG antigen and NP-Pd-HRP-Ab_2 and the results were shown in Fig. 4 (D). The current response increased with the increasing of the incubation time and then leveled off slowly after 60 min, showing an equilibration state. This may be because the interaction between Ab and Ag in the binding sites had reached saturated. Then further increasing incubation time will not affect the change of the current signal. Thus, 60 min was selected as the incubation time for the determination of hCG antigen in this study.

The concentration of H_2O_2 was another important parameter for the immunoassays. As shown in Fig. 4 (E), when the H_2O_2 concentration was less than 0.8 mM, the reduction peak currents increased with increasing H_2O_2 concentration, and then started to level off. The reason is that all the enzyme molecules become saturated with H_2O_2, so the increasing of H_2O_2 concentration does not make much difference. Therefore, 0.8 mM was chosen for the optimal concentration of H_2O_2.

Performance of the immunosensor

A sandwich-type assay format was applied for the detection of hCG by using the synthesized NP-Pd as molecular tags under optimal condition. After hCG molecules were immobilized, they specifically bound to Ab_1, followed by reaction with HRP-Ab_2. In the presence of H_2O_2, HRP (Fe^{2+}) is efficiently converted to its oxidized form, HRP (Fe^{3+}). HRP (Fe^{3+}) is then reduced at the electrode surface. Under a certain condition of H_2O_2 concentration, the reduction current is proportional to the concentration of HRP, thereby indirectly proportional to the concentration of hCG. CV

measurements were recorded in PBS containing 0.8 mM H_2O_2 at a scan rate of 50 mV s^{-1}. The immunosensor was incubated in hCG solution of different concentration. As shown in Fig. 5, the linear relationship between the peak current and the hCG concentration was obtained from 0.5 ng mL^{-1} to 200 ng mL^{-1} with a correlation coefficient of 0.9986. The limit of detection was 9.3 pg mL^{-1}. Therefore, the use of HRP-Ab_2-NP-Pd as detection antibody could significantly amplify the signal through the enzymatic signal amplification of high-content HRP and the presence of NP-Pd on immunosensor surface.

Selectivity, reproducibility and stability of the immunosensor

To evaluate the selectivity of the immunosensor, the effect of interferents was studied on the current responses of the immunosensor in the presence of 20.0 ng mL^{-1} hCG. The interference effects of AFP, CEA, and Vc, etc, were investigated by adding them into the incubation solution. The 20.0 ng mL^{-1} hCG solution containing 50.0 ng mL^{-1} interfering substances was measured by the immunosensor. As shown in Fig. 6, when hCG coexisted with the interferents, no apparent signal change took place in comparision with that of only hCG, which indicated that the system exhibited sufficiently selectivity for the determination of hCG.

Reproducibility of the immunosensor is a key factor for developing a practical immunosensor. The inter-assay precision was estimated by determining the same hCG level with five immunosensors made using the same conditions independently. The relative standard deviations (RSDs) were 4.9%, 4.1%, and 4.6% for 5.0, 20.0 and 50.0 ng mL^{-1} hCG. Similarly, the intra-assay precision was estimated by testing three hCG

levels for five replicate measurements. The RSDs were 5.1%, 4.3% and 3.9% for 5.0, 20.0 and 50.0 ng mL^{-1} hCG. The results obtained were satisfactory.

The stability, another important parameter of immunosensor, was examined by the property of HRP- Ab_2-NP-Pd bioconjugates. When the bioconjugates were not in use, they were stored in PBS (pH 7.2) at 4 ℃. After 3 weeks, the current response of the immunosensor was retained 86% of the initial response. The slow decrease in response might be on account of the gradual deactivation of the immobilized antibody incorporated in the composite. It conformed that the developed immunosensor had excellent stability.

Real sample analysis

To evaluate the applicability of the proposed method, it was used for hCG assay by standard addition methods in human serum. The analytical results were shown in Table 1. The recovery efficiency was in the range of 95.2% –103.45%. Therefore, the proposed immunosensor could be considered as an optional method for detection of hCG in real sample.

Comparison of methods

The proposed method for the determination of hCG was compared with the previously reported methods in Table 2. Compared with previous methods, the proposed method shows relatively higher sensitivity and lower detection limit. The low detection limit might be ascribed to two possible explanations: (□) As discussed earlier, NP-Pd with high surface-to-volume ratio and the high-content HRP exhibited high catalytic efficiency toward the reduction of H_2O_2; (ii) A relatively large amount

of HRP-Ab_2 had been conjugated to NP-Pd label. Usually, when the hCG concentration was low, the amount of hCG captured by Ab_1 immobilized onto the electrode surface was also low. However, the large amount of HRP-Ab_2 immobilized onto the label increases the probability of interactions between HRP-Ab_2 and antigen.

Conclusions

In this study, a new sandwich-type immunoassay protocol for sensitive electrochemical determination of hCG was devised. The NP-Pd with catalytic activity was used for labeling HRP-Ab_2, which could load numerous HRP-Ab_2 to enhance the sensitivity of the immunosensor. The proposed immunosensor showed a wide linear range and satisfactory selectivity, reproducibility and stability. In addition, the proposed strategy provides a biocompatible immobilization and sensitized recognition platform for analytes as small antigens and possesses promising potential in clinical diagnosis.

Acknowledgement

This project was financially supported by Shandong Provincial Natural Science Foundation, China (Grant No. ZR2012BL11), Shandong Provincial Science and Technology Development Plan Project, China (Grant No. 2013GGB01172) and the National Natural Science Foundation of China (Grant Nos. 51003040 and 51102114).

References

1 J. F. Wang, R. Yuan, Y. Q. Chai, S. R. Cao, S. Guan, P. Fu, L. G. Min, *Biochemical Engineering Journal*, 2010, **51**, 95-101.

2 W. Schmidt, K. Klinga, K. Neudeck, B. Runnebaum, F. Kubli, *Geburtshilfe Frauenheilkd*, 1983, **43**, 664-669.

3 Banerjee, N. S. Srilatha, G. S. Murthy, *Biochim. Biophys. Acta.*, 2002, **1569**, 21-30.

4 S. Madersbacher, P. Berger, *Antibodies and immunoassays, Methods*, 2000, **21**, 41-50.

5 H. Sasamoto, M. Maeda, A. Tsuji, H. Manita, *Anal. Chim. Acta.*, 1995, **309**, 221-225.

6 L. X. Zhao, J. M. Lin, F. Qu, *Anal. Chim. Sinica.*, 2004, **62**, 71-77.

7 X. Yan, Z. B. Huang, M. He, X. M. Liao, C. Q. Zhang, G. F. Yin, J. W. Gu, *Colloids and Surfaces B: Biointerfaces.*, 2012, **89**, 86-92.

8 N. Nakamura, T. K. Lim, J. M. Jeong, T. Matsunaga, *Anal. Chim. Acta.*, 2001, **439**, 125-130.

9 Q. P. Qin, M. Christiansen, T. Lovgren, B. Norgaard-Pedersen, K. Pettersson, *J. Immunol. Methods.*, 1997, **205**, 169-175.

10 S. Scsuková, M. Jezová, J. Vranová, M. Tatara, J. Kolena, Gen, *Physiol. Biophys.*, 1996, **15**, 451-462.

11 Y. H. He, Y. P. Li, X. Hun, *Microchimica Acta.*, 2010, **171**, 393-395.

12 J. Y. Hou, T. C. Liu, Z. Q. Ren , M. J. Chen , G. F. Lin, Y. S. Wu, *Analyst*, 2013, **138**, 3697-3704.

13 S. C. Zhang, C. Z. Zhang, Z. Xing, X. R. Zhang, *Clinical Chemistry*, 2004, **50**, 1214-1221.

14 A. H. Liang, M. J. Zou, Z. L. Jiang, *Talanta*, 2008, **75**, 1214-1220.

15 R. Li, D. Wu, H. Li, C.X. Xu, H. Wang, Y.F. Zhao, Y. Y. Cai, Q. Wei, B. Du, *Analytical Biochemistry.*, 2011, **414**, 196-201.

16 J. F. Wang, R. Yuan, Y. Q. Chai, S. R. Cao, S. Guan, P. Fu, L. G. Min. *Biochemical Engineering Journal.*, 2010, **51**, 95-101.

17 R. Chai, R. Yuan, Y. Q. Chai, C. F. Ou, S. R. Cao, X. L. Li, *Talanta*, 2008, **74**, 1330-1336.

18 K. Kerman, N. Nagatani, M. Chikae, T. Yuhi, Y. Takamura, E. Tamiya, *Anal. Chem.*, 2006, **78**, 5612-5616.

19 J. Chen, J. H. Tang, F. Yan, H. X. Ju, *Biomaterials.*, 2006, **27**, 2313-2321.

20 J. Chen, F. Yan, Z. Dai, H. X. Ju, *Biosens. Bioelectron.*, 2005, **21**, 330-336.

21 J. M. Liu, X. M. Huang, M. L. Cui, L. P. Lin, L. H. Zhang, Z. Y. Zheng, *Analytical Biochemistry.*, 2012, **431**, 19-29.

22 Y. L. Cui, H. F. Chen, L. Hou, B. Zhang, B. Q. Liu, G. N. Chen, *Analytica Chimica Acta.*, 2012, **738**, 76-84.

23 C. L. Hong, R. Yuan, Y. Q. Chai, Y. Zhuo, X. Yang, *Journal of Electroanalytical Chemistry,* 2012, **664**, 20-25.

24 B. Zhang, D. P. Tang, B. Q. Liu, Y. L. Cui, H. F. Chen, G. N. Chen, *Analytica Chimica Acta*, 2012, **711**, 17-23.

25 J. P. Lei, H. X. Ju, *Chem. Soc. Rev.*, 2011, **41**, 2122-2134.

26 Z. H. Wen, S. Q. Ci, J. H. Li, *J. Phys. Chem. C.*, 2009, **113**, 13482-13487.

27 G. Pampalakis, S. O. Kelley, *Analyst*, 2009, **134**, 447-449.

28 D. M. Kim, M. A. Rahman, M. H. Do, C. G. Ban, Y. B. Shim, *Biosensors and Bioelectronics*, 2010, **25**, 1781-1788.

29 C. S. Shan, H. F. Yang, J. F. Song, D. X. Han, A. Ivaska, L. Niu, *Anal. Chem.*, 2009, **81**, 2378-2382.

30 T. W. Tsai, G. Heckert, L.F. Neves, Y. Q. Tan, D. Y. Kao, R. G. Harrison, D. E. Resasco, D. W. Schmidtke, *Anal. Chem.*, 2009, 81, 7917-7925.

31 J. F. Wang, R. Yuan, Y. Q. Chai, S. R. Cao, S. Guan, P. Fu, L. G. Min. *Biochemical Engineering Journal*, 2010, **51**, 95-101.

32 W. Sun, Y. Y. Zhang, X. M. Ju, G. G. Li, H. W. Gao, Z. F. Sun, *Analytica Chimica Acta*, 2012, **752**, 39-44.

33 S. Chawla, R. Rawal, S. Sharma, C. Shekhar, Pundir. *Biochemical Engineering Journal*, 2012, **68**, 76-84.

34 S. Chawla, R. Rawal, C. S. Pundir, *Journal of Biotechnology*, 2011, **156**, 39-45.

35 L.F. Liu, O.Albrecht, U. Gosele, *Electrochem. Commun.*, 2010, **12**, 835-838.

36 J. S. Yu, Y. Ding, M.W. Chen, *Chem. Mater.*, 2008, **20**, 4548-4550.

37 X. G. Wang, Z. H. Zhang, *Electrochem. Commun.*, 2009, **11**, 1896-1899.

38 A. H. Liu, H. R. Geng, C. X. Xu, H. J. Qiu, *Analytica Chimica Acta*, 2011, **703**, 172-178.

39 C. X. Xu, Y. Q. Liu, J. P. Wang, H. R. Geng, H. J. Qiu, *Journal of Power Sources*, 2012, **199**, 124-131.

40 C. X. Xu. A. H. Liu, H. J. Qiu, Y. Q. Liu. *Electrochemistry Communication*, 2011, **13**, 766-769.

Figure captions

Fig. 1. (A) SEM and (B) HRTEM images showing the microstructure of NP-Pd; (C) EDS specrum of NP-Pd; (D) Pore size distribution of NP-Pd.

Fig. 2. (A) CVs of (a) bare GCE; (b) GNPs/GCE; (c) PB/GNPs/GCE; (d) GNPs/PB/GNPs/GCE; (B) CVs of (c) Ab_1/GNPs/PB/GNPs/GCE; (b) Ag/Ab_1/GNPs/PB/GNPs/GCE; (a) NP-Pd-HRP-Ab_2/Ag/Ab_1/GNPs/PB/GNPs/GCE. CV conditions: pH 7.2 PBS solution containing 0.2 M KCl and 5 mM $K_3[Fe(CN)_6]$; scan rate: 50 mV s^{-1}.

Fig. 3. The CV response after the sandwich format immunoreaction of the proposed immunosensor in the presence of (A) 100 ng mL^{-1} hCG (B) 150 ng mL^{-1} hCG by using various labels: (a) HRP- Ab_2-NP-Pd, (b) HRP-Ab_2 in pH 7.2 PBS containing 0.8 mM H_2O_2

Fig. 4. Effect of (A) electrochemical reduction time of $HAuCl_4$; (B) the time of forming PB film; (C) pH of PBS; (D) incubation time between Ab and Ag; (E) the substrate (H_2O_2) concentration on the electrochemical response.

Fig. 5. (A) The CVs of the immunosnesor at different concentration of hCG; (B) Calibration plots for hCG solution.

Fig. 6. CVs peak currents of the immunosensor for the detection of (a) hCG, (b) hCG+ Glucose, (c) hCG+ BSA, (d) hCG+ L-Cys, (e) hCG+ L-glutamic acid, (f) hCG+ Folic acid, (g) hCG+ Vc, (h) hCG+ CEA, (i) hCG+ AFP.

Fig. 1

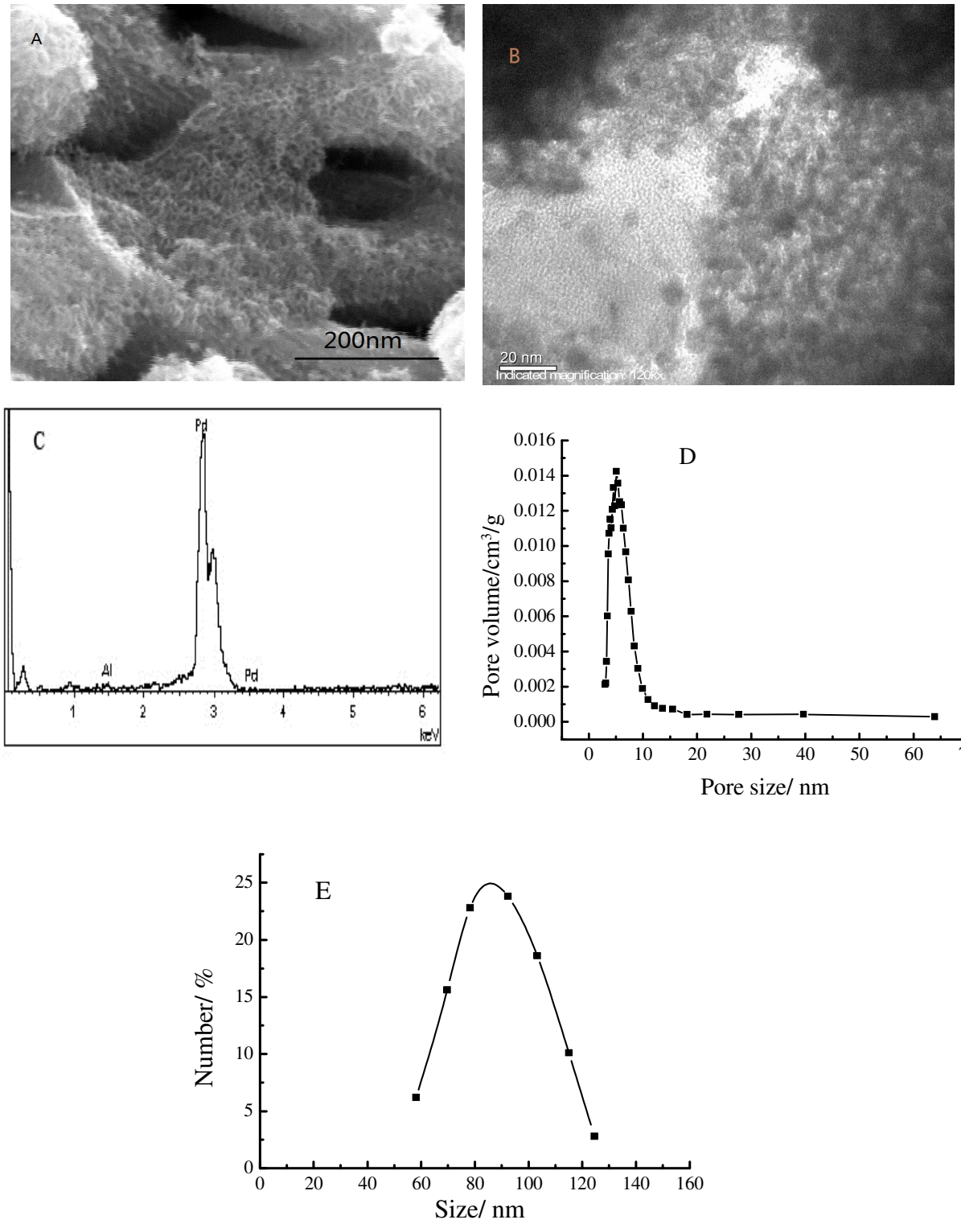

Fig. 2.

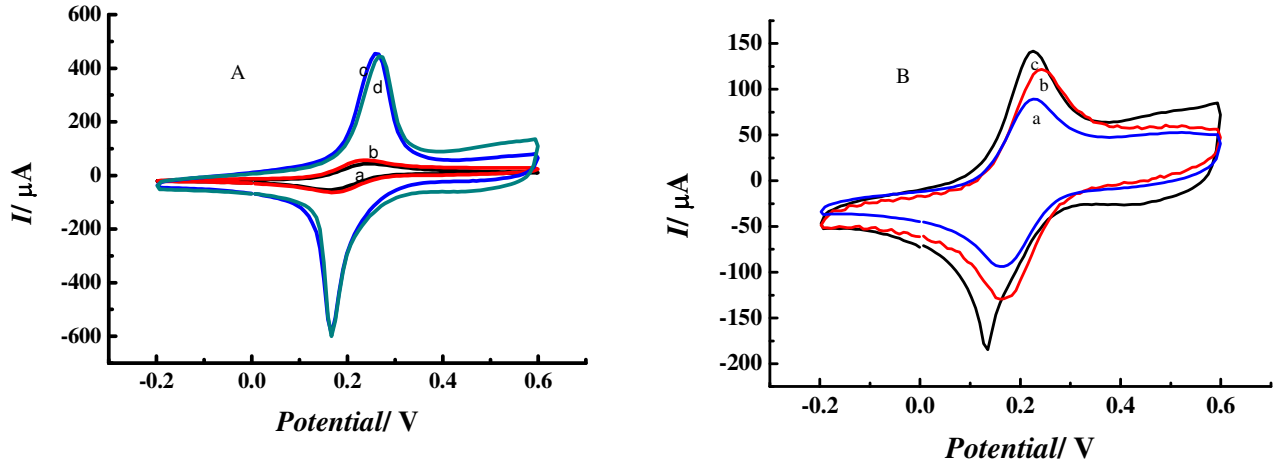

Fig. 3

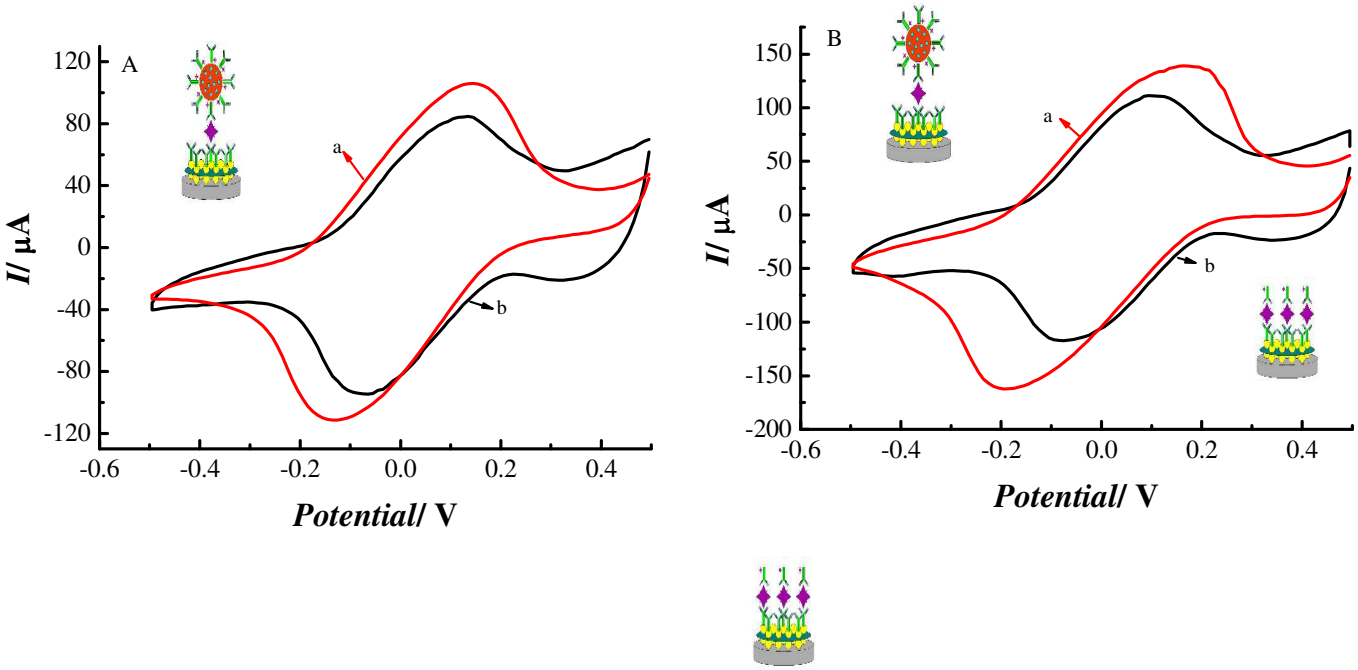

Fig. 4

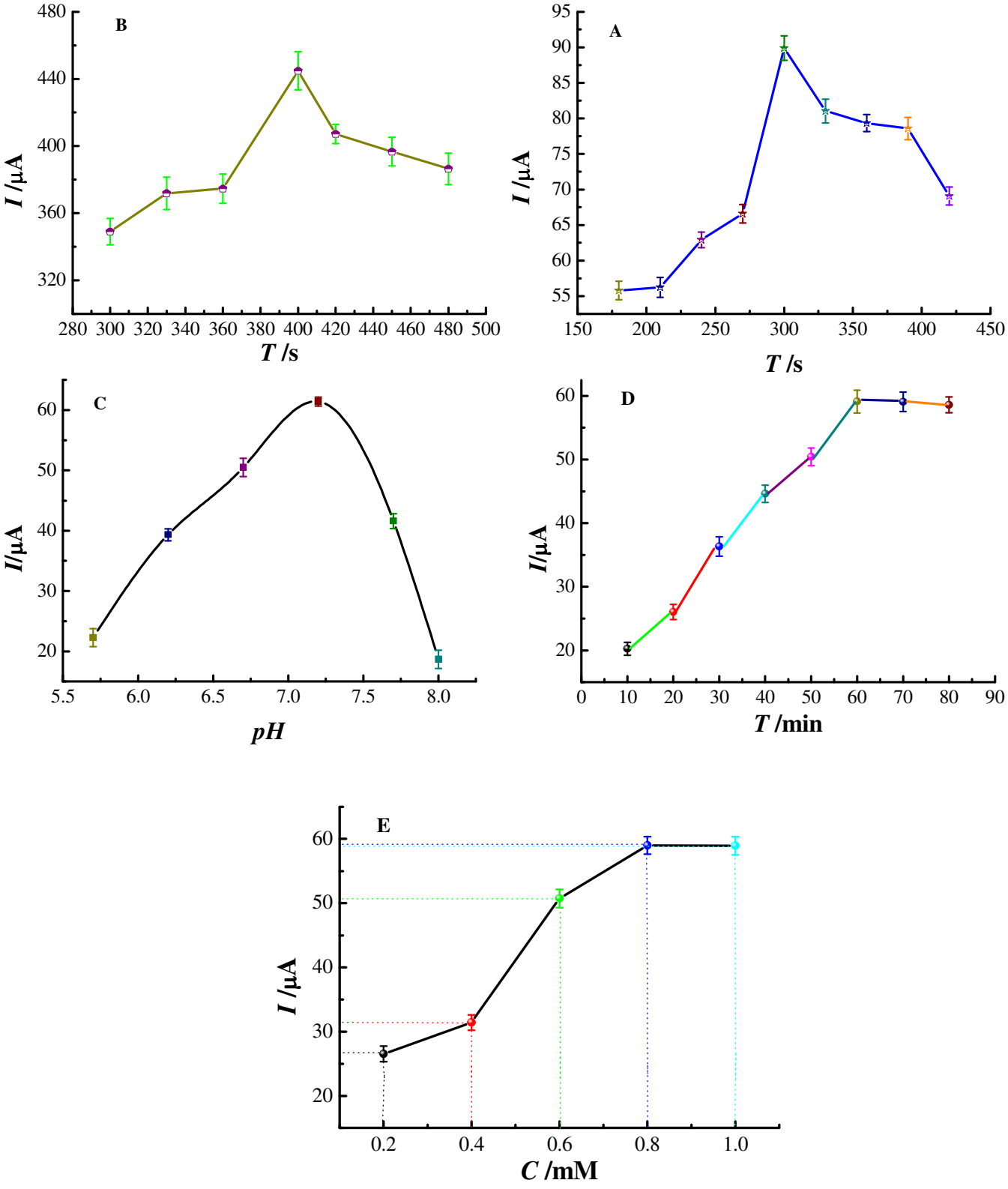

Fig. 5

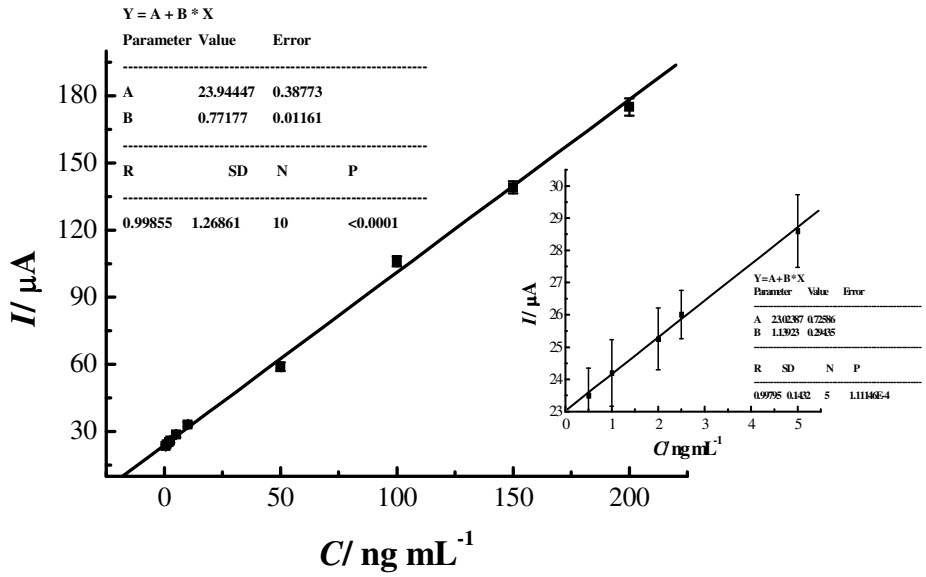

Fig. 6

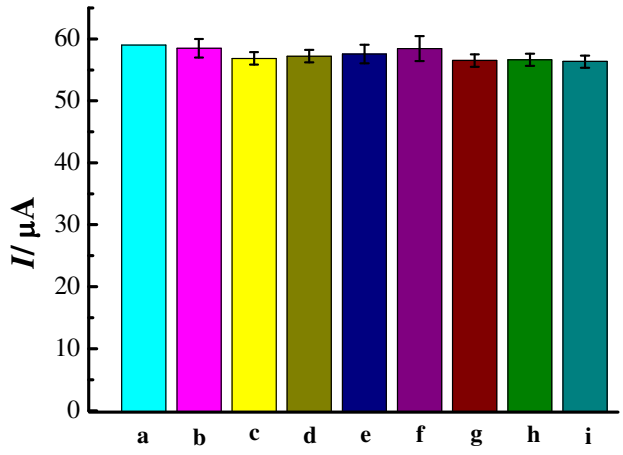

Figure captions

Fig. 1. (A) SEM and (B) HRTEM images showing the microstructure of NP-Pd; (C) EDX specrum of NP-Pd; (D) Pore size distribution of NP-Pd; (E) Grain size distribution of NP-Pd.

Fig. 2. (A) CVs of (a) bare GCE; (b) GNPs/GCE; (c) PB/GNPs/GCE; (d) GNPs/PB/GNPs/GCE; (B) CVs of (c) Ab_1/GNPs/PB/GNPs/GCE; (b) Ag/Ab_1/GNPs/PB/GNPs/GCE; (a) NP-Pd-HRP-Ab_2/Ag/Ab_1/GNPs/PB/GNPs/GCE. CV conditions: pH 7.2 PBS solution containing 0.2 M KCl and 5 mM $K_3[Fe(CN)_6]$; scan rate: 50 mV s^{-1}.

Fig. 3. The CV response after the sandwich format immunoreaction of the proposed immunosensor in the presence of (A) 100 ng mL^{-1} hCG (B) 150 ng mL^{-1} hCG by using various labels: (a) HRP- Ab_2-NP-Pd, (b) HRP-Ab_2 in pH 7.2 PBS containing 0.8 mM H_2O_2

Fig. 4. Effect of (A) electrochemical reduction time of $HAuCl_4$; (B) the time of forming PB film; (C) pH of PBS; (D) incubation time between Ab and Ag; (E) the substrate (H_2O_2) concentration on the electrochemical response.

Fig. 5. (A) The CVs of the immunosnesor at different concentration of hCG; (B) Calibration plots for hCG solution.

Fig. 6. CVs peak currents of the immunosensor for the detection of (a) hCG, (b) hCG+ Glucose, (c) hCG+ BSA, (d) hCG+ L-Cys, (e) hCG+ L-glutamic acid, (f) hCG+ Folic acid, (g) hCG+ Vc, (h) hCG+ CEA, (i) hCG+ AFP.

Table. 1 Determination results of real samples (n=9).

Amount added (ng mL^{-1})	This method (ng mL^{-1} ± RSD%)	Recovery (%)
2.0	1.92 ± 4.87	96
5.0	4.76 ± 3.38	95.2
10.0	10.49 ± 3.25	104.9
50.0	48.76 ± 4.18	97.52
100.0	103.45 ± 2.18	103.45

Table. 2 Comparision of analytical parameters for the determination of hCG

Methods	**Reagents or condition**	**Linear range**	**Detection limit**	**Reference**
Sandwich electrochemical immunosensor	GNPs, PB, NP-Pd	0.5-200 ng mL^{-1} (5-2000 mIU mL^{-1})	9.3 pg mL^{-1} (0.093 mIU mL^{-1})	This paper
Photoluminescence	Hierarchical ZnO arrays	2–160 ng mL^{-1}	-	7
Fluoroimmunoassay	Polymer nanoparticles	1.25-300 mIU mL^{-1}	0.3 mIU mL^{-1}	11
Fluoroimmunoassay	Magnetic particles	0.16-450 ng mL^{-1}	0.08 ng mL^{-1}	12
Spectrometry	an inductively coupled plasma mass spectrometry	5.0–170 ug L^{-1}	1.7 ug L^{-1}	13
Resonance scattering spectral assay	Gold nanoparticles	2.5–208.3 mIU mL^{-1}	0.83 mIU mL^{-1}	14
Immunosensor	Nanoporous gold/ graphene sheets	0.5–40.00 ng mL^{-1}	0.034 ng mL^{-1}	15
Immunosensor	Gold nanoparticles/ poly-(2,6-pyridinediamine)/multiwall carbon nanotubes	1-160.0 mIU mL^{-1}	0.3 mIU mL^{-1}	16
Immunosensors	gold nanoparticles/ methylene blue/thiourea	1.0–100.0 mIU mL^{-1}	0.3 mIU mL^{-1}	17

Graphical abstract

GNPs/PB/GNPs and NP-Pd were prepared to immobilized Ab_1 and HRP-Ab_2 respectively and combined to construct a sandwich-type immunosnesor for hCG.